Classical Dynamics near the Triple Collision in a Three-Body Coulomb Problem

Nark Nyul Choi,[1] Min-Ho Lee,[1] and Gregor Tanner[2]

[1]*School of Natural Science, Kumoh National Institute of Technology, Kumi, Kyungbook 730-701, Korea*
[2]*School of Mathematical Sciences, University of Nottingham, University Park, Nottingham NG7 2RD, United Kingdom*

We investigate the classical motion of three charged particles with both attractive and repulsive interactions. The triple collision is a main source of chaos in such three-body Coulomb problems. By employing the McGehee scaling technique, we analyze here for the first time in detail the three-body dynamics near the triple collision in 3 degrees of freedom. We reveal surprisingly simple dynamical patterns in large parts of the chaotic phase space. The underlying degree of order in the form of approximate Markov partitions may help in understanding the global structures observed in quantum spectra of two-electron atoms.

PACS numbers: 45.50.Tn, 05.45.Mt

Our understanding of the overall dynamics of gravitational or Coulomb three-body problems is still very limited. This can be attributed to the large dimensionality of the systems, the long range interactions, and the complexity of the dynamics near the nonregularizable triple collision [1]. The latter singularity dominates, in particular, the dynamics in three-body Coulomb problems such as two-electron atoms. Wannier's threshold law [2], as well as experimental results on double ionization due to single [3] or multiple [4] photon processes, shows electron-electron correlation effects that are linked to near triple collision events [5,6]. The excitation of two single-electron wave packets in two-electron atoms has recently been achieved experimentally, making it possible to study classical collision events quantum mechanically [7]. The importance of the triple collision on quantum spectra of two-electron atoms is also evident from semiclassical treatments restricted to collinear subspaces of the full dynamics [8].

We present here for the first time a comprehensive analysis of the classical dynamics near the triple collision in two-electron atoms in the full $L = 0$ phase space. Previous work has been restricted to low dimensional invariant subspaces such as collinear configurations or the so-called Wannier ridge [8–12]. We start by describing the dynamics *at* the triple collision in 3 degrees of freedom. The topology of the singularity together with the particle exchange symmetry strongly affects the scattering signal for energies below the three-particle breakup energy. We derive new scaling laws similar to the Wannier threshold law [2] and show for the first time that large parts of the phase space are highly structured in terms of approximate Markov partitions. This is an important step towards analyzing electron-electron correlation effects found in quantum properties of two-electron atoms [8] in terms of the overall phase space dynamics.

Working in the infinite nucleus mass approximation and restricting ourselves to angular momentum $L = 0$,

the dynamics may be described in terms of the hyper-radius $R = (r_1^2 + r_2^2)^{1/2}$, the hyperangle $\alpha = \tan^{-1}(r_2/r_1)$ with $r_{1,2}$ being the electron-nucleus distances, and the interelectronic angle θ. Following McGehee [9,13], we formally remove the triple collision singularity by employing a scaling transformation with respect to $R(t)$ according to $p_R \rightarrow \sqrt{R}\, p_R$, $p_{\alpha,\theta} \rightarrow p_{\alpha,\theta}/\sqrt{R}$, and $dt \rightarrow dt/R^{3/2}$ resulting for two-electron systems in equations of motion of the form

$$\dot{\alpha} = p_\alpha, \qquad \dot{p}_\alpha = -\frac{1}{2}p_R p_\alpha - \frac{\partial}{\partial\alpha}\bar{H}, \qquad \dot{\theta} = \frac{\partial}{\partial p_\theta}\bar{H},$$

$$\dot{p}_\theta = -\frac{1}{2}p_R p_\theta - \frac{\partial}{\partial\theta}\bar{H}, \qquad \dot{\bar{H}} = p_R\bar{H}, \qquad (1)$$

$$\dot{p}_R = \frac{1}{2}p_\alpha^2 + \frac{1}{2}\frac{p_\theta^2}{\cos^2\alpha\sin^2\alpha} + \bar{H},$$

where

$$\bar{H} = \frac{1}{2}\left(p_R^2 + p_\alpha^2 + \frac{p_\theta^2}{\cos^2\alpha\sin^2\alpha}\right) + V(\alpha,\theta) = RE,$$

$$V = -Z(1/\cos\alpha + 1/\sin\alpha) + 1/\sqrt{1 - \sin2\alpha\cos\theta}, \qquad (2)$$

and Z is the charge of the nucleus; we will use $Z = 2$ throughout if not stated otherwise. The hyper-radius has been eliminated from the scaled differential Eqs. (1) and $R(t)$ is now given implicitly through (2). The triple collision itself has been removed and the remaining singularities due to two-body collisions at $\alpha = 0, \pi/2$ can be regularized using the Kustaanheimo-Stiefel transformation [10,14].

There are two fixed points of the dynamics (1),

$$\alpha = \pi/4, \qquad \theta = \pi, \qquad p_\alpha = p_\theta = 0, \qquad p_R = \pm P_0,$$

where $P_0 = [\sqrt{2}(4Z - 1)]^{1/2}$. These fixed points correspond to trajectories in the unscaled phase space where both electrons fall into the nucleus symmetrically along the collinear axis, that is, the *triple collision point* (TCP)

with $p_R = -P_0$ and its time reversed partner, the trajectory of symmetric double escape, the *double escape point* (DEP) with $p_R = P_0$. A true reduction in the dimensionality (from 5 to 4) of the problem is achieved for the special initial condition $\bar{H} = 0$ for which $\bar{H}$ becomes a constant of motion. The $\bar{H} = 0$ subspace that contains the two fixed points corresponds to $R = 0$ *or* $E = 0$, that is, to the dynamics at the triple collision or equivalently to the dynamics at $E = 0$. We will come back to this remarkable fact when studying the transition from $E = 0$ to the dynamics for $E < 0$. There are three invariant subspaces of the dynamics: the collinear spaces $\theta = \pi$, $p_\theta = 0$ (the *eZe* configuration) and $\theta = 0$, $p_\theta = 0$ (the *Zee* configuration) as well as the so-called Wannier ridge (WR) of symmetric electron dynamics, $\alpha = \pi/4$, $p_\alpha = 0$. The *eZe* configuration and the Wannier ridge are connected at the fixed points.

Linearizing the dynamics near the DEP reveals that two of the five eigendirections, $\mathbf{v}^{(1,2)}$, lie in the WR with eigenvalues $\lambda_D^{(1,2)} = -[1 \pm \sqrt{(4Z-9)/(4Z-1)}\,]P_0/4$; the other three eigenvectors, $\mathbf{v}^{(3,4,5)}$, lie in the *eZe* space with $\lambda_D^{(3,4)} = -[1 \pm \sqrt{(100Z-9)/(4Z-1)}\,]P_0/4$ and $\lambda_D^{(5)} = P_0$, where the subscript D refers to DEP [2]. The unstable manifold $U_D^{(5)}$ along the $\mathbf{v}^{(5)}$ direction is oriented along $-p_R$ leading out of the $E = 0$ subspace; the unstable manifold $U_D^{(4)}$ lies in $E = 0$ and corresponds to a trajectory leaving the DEP towards $p_R = \infty$. The 3D stable manifold S_D including $S_D^{(i)}$ associated with $\mathbf{v}^{(i)}$ ($i =$

FIG. 1 (color online). The PSOS $\theta = \pi$ of the $E = 0$ manifold in α-$\bar{p}_\alpha$-p_R coordinates ($Z = 2$). The *eZe* space forms the boundary of the PSOS, the WR connects the TCP and DEP fixed points; below, various cuts of the PSOS at fixed p_R values are shown together with the S_D. The two arms of the S_D stretching from the WR towards the $S_D^{(3)}$ on the *eZe* boundary are shown as full and dashed lines, respectively. (The S_D in C-E is drawn schematically to enhance important features.)

1, 2, 3) is embedded in the 4D $E = 0$ subspace. In what follows the structure of the S_D is of special importance being responsible for the striking features in the classical electron-impact scattering signal for total energy $E < 0$. (From time reversal symmetry, one obtains for the TCP $\lambda_T^{(i)} = -\lambda_D^{(i)}$ for $i = 1$–5. The manifolds $U_T^{(1,2,3)}$ and $S_T^{(4,5)}$ can be obtained from the corresponding $S_D^{(1,2,3)}$ and $U_D^{(4,5)}$, respectively.)

We analyze first the topology and the dynamics in the triple-collision phase space $E = 0$ focusing especially on the structure of the S_D. The *topology* of the space $E = 0$ is most conveniently studied by considering the 3D Poincaré surface of section (PSOS) $\theta = \pi$ in α-p_α-p_R coordinates. From (2), one obtains that the *eZe* configuration forms the boundary of the PSOS; see Fig. 1. A typical scattering event follows a trajectory coming from infinity with $p_R = -\infty$, $\alpha = 0$ or $\pi/2$ and one of the two electrons leaving towards infinity with $p_R \to \infty$, $\alpha \to \pi/2$ or 0. After lifting the singularity at $\alpha = 0$ or π by considering $\bar{p}_\alpha = p_\alpha \sin 2\alpha$, the topology of the *eZe* phase space takes on the form of a sphere with four points taken to $|p_R| = \infty$; see Fig. 1 [9]. The two fixed points are located at the saddles between the arms stretching in forward and backward directions along the p_R axis. The WR space connects the TCP and DEP along the axis $\alpha = \pi/4$, $\bar{p}_\alpha = 0$; see Fig. 1. It is a compact manifold with the topology of a S^2 sphere where the fixed points form opposite poles.

For $\bar{H} = 0$, we have $\dot{p}_R \geq 0$, which leads to a relatively simple overall dynamics. Its important features can be characterized by the behavior of the stable or unstable manifolds of the fixed points. Various cuts of the S_D in the PSOS for fixed $p_R < P_0$ are shown in Fig. 1. The S_D is for $-P_0 \leq p_R \leq P_0$ bounded by the 1D stable manifold $S_D^{(3)}$ in the *eZe* space, and the 2D WR. That is, the S_D is the stable manifold of the WR. What makes the evolution of this manifold remarkable is its behavior at the TCP at $p_R = -P_0$, where the phase space itself splits into two distinct parts. Starting at $p_R = P_0$ and going towards decreasing p_R values, which corresponds essentially to an evolution of the S_D backwards in time, the S_D undergoes the usual stretching and folding mechanism typical for an unstable manifold in compact domains. The stretching and folding is here facilitated by an overall rotation of the space around the WR axis $\alpha = \pi/4$, $\bar{p}_\alpha = 0$ and a certain "stickiness" near the binary collision points $\alpha = 0$ or $\pi/2$; see the cuts **B** and **C** in Fig. 1 [14]. As $p_R \to -P_0$, the phase space develops a bottleneck, whereas the S_D stretches over the whole phase space 5 times by now. As p_R decreases further passing through $-P_0$, the S_D is cut at the TCP into distinct parts; see **D** in Fig. 1. The TCP itself, however, is not part of S_D. Points close to the TCP leave the fixed point along the stable manifold $S_T^{(4)}$ in *eZe* space towards $p_R \to -\infty$. In each arm exactly five pieces of the S_D come together at the $S_T^{(4)}$ for $p_R < -P_0$ forming two loops and one connection to
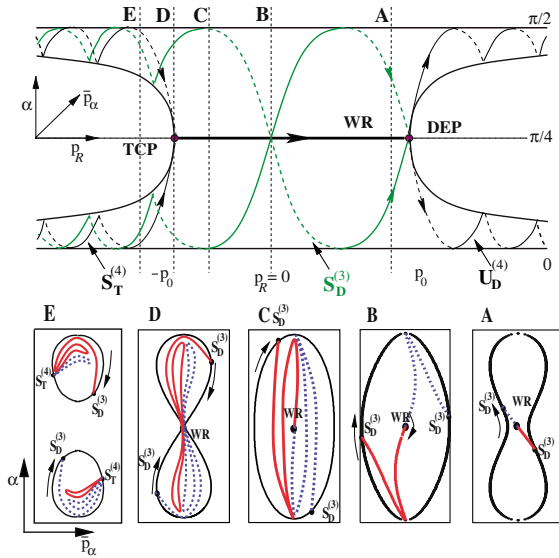
the eZe boundary; see Fig. 1E. The $S_T^{(4)}$ is thus *not* part of the S_D, but forms a boundary of that manifold. (The $S_T^{(4)}$ can in this sense be regarded as the preimage of the heteroclinic intersections of the U_T and S_D occurring for $p_R > -P_0$.) There are therefore two main routes towards the DEP for electrons coming in from $p_R = -\infty$ close to the eZe boundary: the first route approaches the TCP on one of the five leaves of the S_D close to the stable manifold $S_T^{(4)}$ and moves then along the WR towards the DEP; second, trajectories can approach the DEP "directly" by moving on the S_D in the vicinity of the $S_D^{(3)}$. This twofold approach is essential for understanding the dynamics in the $E < 0$ space.

We now turn to the full dynamics in the 5D $E < 0$ phase space. We analyze one-electron scattering signals where electron 1, say, starts at $r_1 = \infty$ with energy E_1 and fixed total energy $E = -1$. We record the time delay of the outgoing electron. (Note that fixing $E = -1$ is sufficient as changing the total energy amounts to a simple scaling transformation in the dynamics [10].) A smooth transition of the dynamics from $E < 0$ towards $E = 0$ is achieved by considering the limit $E_1 \to \infty$, $E_2 \to -\infty$ and $E_1 + E_2 = -1$. The inner electron is then initially bounded infinitely deeply in the Coulomb well, and interactions between the incoming and bound electrons take place at $R \to 0$ and thus $\bar{H} \to 0$. The dynamics in $E = 0$ is in this sense equivalent to the dynamics at the triple collision point $R = 0$, and the phase space flow at $E = 0$ can be smoothly continued to the flow in the full $E \neq 0$ space. Trajectories close to $\bar{H} = 0$ follow the dynamics in the triple collision space except near the fixed points where the flow close to the manifold $E = 0$ is perpendicular to that manifold along $\mathbf{v}^{(5)} = -p_R$.

In Fig. 2, a typical signal for the scattering time τ is shown, here for $\theta = \pi/2$ and $E_1 = 0.2$, where θ is the interelectronic angle for $r_1 \to \infty$. (We have chosen zero

FIG. 2 (color online). The time-delay signal for $\theta = \pi/2$ and $E_1 = 0.2$; five distinct peaks appear in the "dips" associated with close encounters with the triple collision point. Note that delay times are shown on logarithmic scales.

angular momentum of both electrons initially). $\varphi \in [-\pi, \pi]$ parametrizes the starting point along one revolution of the trajectory of the inner electron. Disregarding the finer structures of the signal at the moment, two main features emerge, a dip in the scattering time around $\varphi = -1.0$ and a chaotic scattering interval (CSI) around $0.2 < \varphi < 2.2$. The dip can be associated with trajectories close to S_T near $S_T^{(4)}$, which move towards the TCP. Most of these events lead to immediate, fast ionization of one of the two electrons due to the large momentum transfer possible near the triple collision singularity causing the dip in the scattering time. Note that the 2D stable manifold S_T is completely embedded in the eZe configuration; it is not possible to reach the TCP from outside the eZe region.

Chaotic scattering occurs, on the other hand, if trajectories approach the DEP close to the stable manifold S_D via the direct route near $S_D^{(3)}$. The 3D stable manifold of the DEP is part of the $E = 0$ space, and the DEP can thus be reached for $E < 0$ only in the limit $E_1 \to \infty$. Orbits close to the $S_D^{(3)}$ will, however, also come close to the DEP where they either follow $U_D^{(4)}$ leading to ionization or follow $U_D^{(5)}$ along the p_R axis perpendicular to the $\bar{H} = 0$ manifold. In the latter case, $\dot{p}_R$ changes sign and electron trajectories fall back towards the nucleus having equidistributed their momenta in such a way that chaotic scattering becomes possible. The DEP thus acts as a turnstile for entering into a *chaotic scattering region* of the full phase space. By time-reversal symmetry, the TCP acts as the exit gate for single electron ionization.

A closer analysis of the strongly fluctuating signal in the CSI reveals a series of dips flanked by singularities in the delay time on either side; see Fig. 2. The dips correspond to orbits, which, after having spent some time in chaotic motion, leave the chaotic region by coming close to the TCP along the stable manifold $S_T^{(5)}$. The borders of these intervals are given by orbits escaping asymptotically with zero kinetic energy of the outgoing electron. All these escaping regions can be labeled uniquely by a finite binary code reflecting the order in which binary near-collision events take place after entering and before escaping the chaotic region. The mechanisms leading to escape and to the existence of a binary symbolic dynamics forming a complete Smale horseshoe are well documented and understood for the eZe configuration [9,10]. It is surprising that this mechanism holds in principle also far away from the eZe regime down to initial interelectronic angles of the order $\theta \approx \pi/4$.

There is one major difference between the scattering signal for the collinear eZe space and the dynamics for $\theta \neq \pi$: additional structures emerge at the center of the dips; see Fig. 2. When enlarging the regions near the dips both at the primary dip and in the CSI, one finds five separate peaks and, on further magnification, each of these peaks breaks up into a chaotic scattering signal
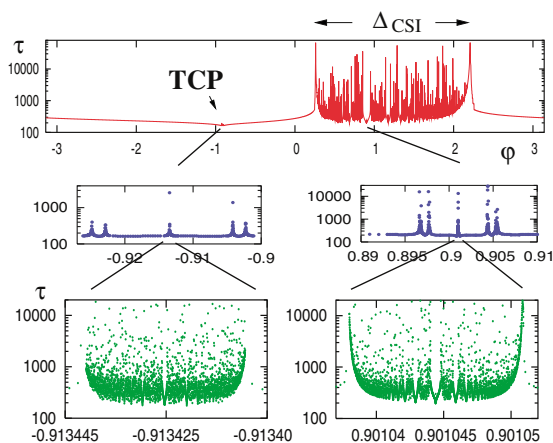
similar to the primary pattern. One finds in this way a whole sequence of self-similar structures where dips give birth to CSI's which in turn have second generation dips containing five peaks, etc. Such a sequence leading up to the second generation CSI is shown in Fig. 2.

These phenomena can be explained in terms of the dynamics in the triple collision space $\bar{H} = 0$ discussed earlier. The dips represent close encounters with the TCP; whereas in the eZe space, the only route away from the TCP is along the unstable manifold $U_T^{(3)}$, for $\theta \neq \pi$ another route opens up: escape along the WR and thus along parts of the S_D leading back to the DEP and to reinjection into the chaotic scattering region. The existence of the five peaks in each of the dips is thus a clear manifestation of the stretching, folding, and cutting mechanism of the S_D in the $\bar{H} = 0$ dynamics. A closer analysis reveals that the center peak (CP) of the five peaks corresponds to the part of the S_D connected to the WR; the outer peaks contain orbits which move away from the WR after passing the TCP and before entering the DEP region. By repeatedly moving from the DEP to the exit channel, the TCP, and then along the WR back to the DEP, it is possible to create increasingly longer cycles of chaotic scattering events. We do thus encounter here a rather curious dynamical feature, namely, a Smale horseshoe, whose entrance and exit points are short circuited by a degenerate heteroclinic manifold, the WR, connecting the two fixed points sitting at these turnstile gates.

The features described above imply scaling laws for the width Δ of the CSI's for $E_1 \rightarrow \infty$. In this limit, trajectories that will enter the chaotic scattering region along $U_D^{(5)}$ need to come closer and closer to the DEP. The size of this phase space region near the DEP is limited by ejection along $U_D^{(4)}$. A simple estimate yields $\Delta \sim E_1^{-\mu}$ with $\mu = \lambda_D^{(4)}/\lambda_D^{(5)}$. The *universality* of this scaling law for both primary and secondary CSI's is shown in Fig. 3 and demonstrates that the DEP is indeed the sole entrance gate into the chaotic scattering region. The exponent μ is the so-called Wannier exponent, which plays a crucial role in Wannier's threshold law for $E > 0$ [2] and is also of importance for quantum resonance widths [15]. A similar scaling law can be deduced for the CP; the phase space volume that can be transferred from the TCP to the DEP along the WR scales in the eZe limit $\theta \rightarrow \pi$ like $\Delta_{CP} \sim (\pi - \theta)^\nu E_1^{-\mu}$ with $\nu = \lambda_T^{(3)}/\mathrm{Re}[\lambda_T^{(1)}] = \lambda_D^{(3)}/\mathrm{Re}[\lambda_D^{(1)}]$; see Fig. 3.

Our analysis suggests that the Markov partition leading to the symbolic dynamics of the eZe space remains largely intact over a substantial part of the $L = 0$ phase space with the only modification that the number of symbols increases from 2 to at least $2 + 5 = 7$. The existence of such a partition in this high-dimensional prob-
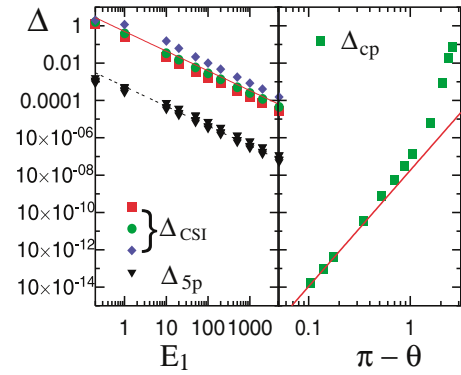

FIG. 3 (color online).   Energy scaling of both the widths of the primary CSI Δ_{CSI} (see Fig. 2) for $\theta = \pi$, $\pi/2$, and $\pi/3$, as well as the widths of the five peaks Δ_{5p} (here for $\theta = \pi/2$), is shown; the scaling agrees with $\mu = 1.0558932\ldots$ for $Z = 2$. To the right, the width, Δ_{CP}, of the center peak of the five peaks is shown as a function of $\pi - \theta$ (for fixed E_1) with scaling exponent $\nu = 6.223573\ldots$.

lem is not obvious and may be the key for explaining long range electron-electron correlation effects and ultimately approximate quantum numbers observed in two electron atoms [8].

[1] F. Diacu and P. Holmes, *Celestial Encounters: The Origins of Chaos and Stability* (Princeton University Press, Princeton, NJ, 1997).
[2] G. H. Wannier, Phys. Rev. **90**, 817 (1953); J. M. Rost, Phys. Rep. **297**, 271 (1998).
[3] R. Doerner *et al.*, Phys. Rep. **330**, 95 (1998).
[4] Th. Weber *et al.*, Nature (London) **405**, 658 (2000).
[5] B. Eckhardt and K. Sacha, Phys. Scr. **T90**, 185 (2001).
[6] T. Schneider and J. M. Rost, Phys. Rev. A **67**, 062704 (2003).
[7] S. N. Pisharody and R. R. Jones, Science **303**, 813 (2004).
[8] G. Tanner *et al.*, Rev. Mod. Phys. **72**, 497 (2000).
[9] Z.-Q. Bai, Y. Gu and J. M. Yuan, Physica D (Amsterdam) **118**, 17 (1998); M. M. Sano, J. Phys. A **37**, 803 (2004).
[10] K. Richter *et al.*, Phys. Rev. A **48**, 4182 (1993).
[11] K. Richter and D. Wintgen, J. Phys. B **23**, L197 (1990).
[12] K. Richter and D. Wintgen, Phys. Rev. Lett. **65**, 1965 (1990); B. Duan *et al.*, Phys. Rev. A **61**, 062711 (2000).
[13] R. McGehee, Inventiones Mathematicae **27**, 191 (1974).
[14] N. N. Choi, M.-H. Lee, and G. Tanner (to be published).
[15] J. M. Rost and D. Wintgen, Europhys. Lett. **35**, 19 (1996).